The biomechanical, chemical, and physiological adaptations of the eggs of two Australian megapodes to their nesting strategies and their implications for extinct titanosaur dinosaurs

Gerald Grellet-Tinner, Suzanne Lindsay, Mike Thompson

Megapodes are galliform birds endemic to Australasia and unusual amongst modern birds in that they bury their eggs for incubation in diverse substrates and using various strategies. *Alectura lathami* and *Leipoa ocellata* are Australian megapodes that build and nest in mounds of soil and organic matter. Such unusual nesting behaviors have resulted in particular evolutionary adaptations of their eggs and eggshells. We used a combination of scanning electron microscopy, including electron backscatter diffraction and energy-dispersive X-ray spectroscopy, to determine the fine structure of the eggshells and micro-CT scanning to map the structure of pores. We discovered that the surface of the eggshell of *A. lathami* displays nodes similar to those of extinct titanosaur dinosaurs from Transylvania and Auca Mahuevo egg layer #4 (AM L#4). We propose that this pronounced nodular ornamentation is an adaptation to an environment rich in organic acids from their nest mound, protecting the egg surface from chemical etching and leaving the eggshell thickness intact. By contrast, *L. ocellata* nests in mounds of sand with less organic matter in semiarid environments and has eggshells with weakly defined nodes, like those of extinct titanosaurs from AM L#3 that also lived in a semiarid environment. We suggest the internode spaces in both megapode and titanosaur species act as funnels, which concentrate the condensed water vapor between the nodes. This water funneling in megapodes through the layer of calcium phosphate reduces the likelihood of bacterial infection by creating a barrier to microbial invasion. In addition, the accessory layer of both species possesses sulfur, which reinforces the calcium phosphate barrier to bacterial and fungal contamination. Like titanosaurs, pores through the eggshell are Y-shaped in both species, but *A. lathami* displays unique mid-shell connections tangential to the eggshell surface and that connect some adjacent pores, like the eggshells of titanosaur of AM L#4 and Transylvania. The function of these inter-connections is not known, but likely helps the diffusion of gases in eggs buried in environments where occlusion of pores is possible.

The biomechanical, chemical, and physiological adaptations of the eggs of two Australian megapodes to their nesting strategies and their implications for extinct titanosaur dinosaurs

Gerald Grellet-Tinner[1,2], Suzanne Lindsay[3], Michael B. Thompson[4]

[1]CONICET, CRILAR, Anillaco, La Rioja, Argentina

[2]The Orcas Island Historical Museums, Eastsound, WA, USA

[3]The Australian Museum, 6 College Street, Sydney
NSW 2010, Australia

[4]School of Biological Sciences, Heydon-Laurence Building (A08), University of Sydney, NSW 2006, Australia

Running title: Adaptations of megapode eggs

[2]Correspondence to
Gerald Grellet-Tinner
The Orcas Island Historical Museums,
Eastsound, WA, USA
CONICET Investigador Correspondiente,
Anillaco, La Rioja, Argentina;
Tel: 360 298 20 55
Email: locarnolugano@gmail.com

19 The authors declare no competing interests.

Abstract

Megapodes are galliform birds endemic to Australasia and unusual amongst modern birds in that they bury their eggs for incubation in diverse substrates and using various strategies. *Alectura lathami* and *Leipoa ocellata* are Australian megapodes that build and nest in mounds of soil and organic matter. Such unusual nesting behaviors have resulted in particular evolutionary adaptations of their eggs and eggshells. We used a combination of scanning electron microscopy, including electron backscatter diffraction and energy-dispersive X-ray spectroscopy, to determine the fine structure of the eggshells and micro-CT scanning to map the structure of pores. We discovered that the surface of the eggshell of *A. lathami* displays nodes similar to those of extinct titanosaur dinosaurs from Transylvania and Auca Mahuevo egg layer #4 (AM L#4). We propose that this pronounced nodular ornamentation is an adaptation to an environment rich in organic acids from their nest mound, protecting the egg surface from chemical etching and leaving the eggshell thickness intact. By contrast, *L. ocellata* nests in mounds of sand with less organic matter in semiarid environments and has eggshells with weakly defined nodes, like those of extinct titanosaurs from AM L#3 that also lived in a semiarid environment. We suggest the internode spaces in both megapode and titanosaur species act as funnels, which concentrate the condensed water vapor between the nodes. This water funneling in megapodes through the layer of calcium phosphate reduces the likelihood of bacterial infection by creating a barrier to microbial invasion. In addition, the accessory layer of both species possesses sulfur, which reinforces the calcium phosphate barrier to bacterial and fungal contamination. Like titanosaurs, pores through the eggshell are Y-shaped in both species, but *A. lathami* displays unique mid-shell connections tangential to the eggshell surface and that connect some adjacent pores, like the eggshells of titanosaur of AM L#4 and Transylvania. The function of these inter-connections is not known, but likely helps the diffusion of gases in eggs buried in environments where occlusion of pores is possible.

Introduction

Megapodes are galliform birds endemic to Australia and islands in Indonesia, Papua New Guinea and Oceania (Del Hoyo et al., 1994; Jones et al., 1995; Sibley and Monroe, 1990; Göth, and Vogel, 1997). Together, Galliformes and its Anseriformes sister taxon form an evolutionarily significant lineage that is the sister group to all remaining modern birds (Del Hoyo et al., 1994; Jones et al., 1995; Paganelli, 1980). Although phylogenetics imply that the root of the megapode lineage should be in the Late Cretaceous, the earliest Megapodiidae fossil record dates only from the late Oligocene (ca. 25 million years ago) of Lake Pinpa, northern South Australia (Boles and Ivison, 1999). Equally bewildering, the internal phylogenetic relationships of the 22 or so extant megapode species classified in six or seven genera was still debated (Del Hoyo et al., 1994; Jones et al., 1995; Birks and Edwards, 2002; Dekker and Brom, 1992) until recently when two molecular-based (using nuclear and mitochondrial DNA) phylogenetic analyses (Birks and Edwards, 2002; Harris et al., 2014) seem to have clarified the internal phylogeny of these birds.

The incubation strategies of megapodes are atypical of modern birds as they rely on heat from the nest for incubation, like the Cretaceous sauropods (Hechenleitner et al., 2015), rather than heat transfer from the brood patch of the incubating bird. Presently, the megapodes display the following five unusual nesting behaviors (Frith, 1956; Del Hoyo et al., 1994; Jones et al., 1995): *1. mound-building using soil and vegetation; 2. burrow-nesting using geothermal sites; 3. burrow-nesting using solar-heated beaches; 4. burrow-nesting using decaying tree roots; 5. mound parasitism.* When and how these homoplastic incubation behaviours re-evolved is unknown and which among the five strategies is the most primitive remains unclear. All living Australian megapodes (3 species, 3 genera) build mounds. Here we describe the functional morphology of the eggs and eggshells of two most common Australian megapodes: the Australian brush turkey *(Alectura lathami)* and mallee fowl *(Leipoa ocellata)*, particularly as it relates to

their incubations in mounds. *Leipoa ocellata* occurs mostly in semi-arid environments and dryland mallee habitats (Fig. 1) in inland areas of southern Australia, while *Alectura lathami* is distributed along the east coast of Australia from Cape York to the Sydney, an area of coastal humid weather that contrasts to the arid to semi-arid habitat of the mallee fowl (Fig. 1).

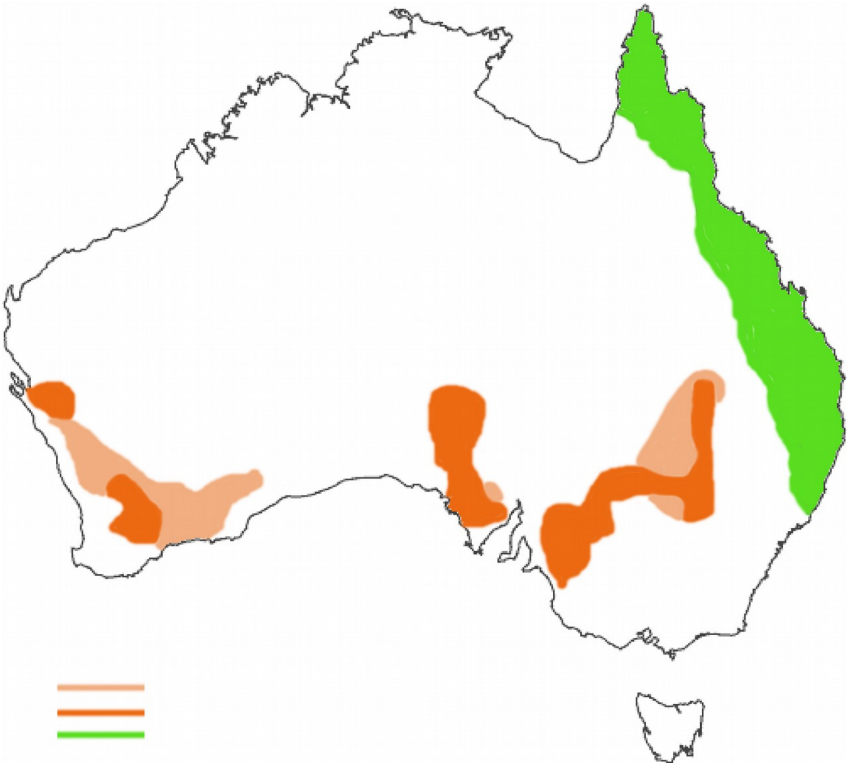

*Figure 1: Distribution of the Australian brush turkey (*Alectura lathami*) and the current (dark orange) and historical (light orange) distributions of the mallee fowl (*Leipoa ocellata*).* Alectura lathami *thrives in the wetter eastern coastal regions* (Frith, 1979) *while* L. ocellata *lives in dry environments* (Frith, 1959; Booth, 1987a).

Abbreviations

ACMM: Australian Centre for Microscopy and Microanalysis

AM: The Australian Museum

EBSD: Electron backscatter diffraction

EDS: Energy-dispersive X-ray spectroscopy

SEM: Scanning electron microscopy

BSEM: Back-scattered electron microscopy

BC (band contrast): A measure of the quality of the diffraction pattern at each point, showing the level of contrast within the Kikuchi bands in the patterns. A higher value (brighter shade of grey) indicates stronger diffraction at that point.

FSD (forescatter detectors): A detector system or image type that is generated by backscattered electrons that are scattered in a forward direction (i.e. down the tilted surface) towards detectors mounted below the EBSD detector phosphor screen in the scanning electron microscope. These images are dominated by both topography on the sample surface and channeling contrast, in which regions with different crystallographic orientation generate different contrast levels.

IPFX (inverse pole figure X): A colouring scheme for orientation maps, showing which crystal direction is parallel to the Map X direction (i.e. normal to the shell surface). The attached colour scheme is needed to see which crystal direction is represented by which colour (e.g. if the point is coloured in red, it means that the c-axis (001) of the calcite crystal is parallel to the x direction).

Description

Leipoa ocellata lays oval to elongated oval-shaped eggs rather than the typical pear to oval shape observed in most galliform and anseriform birds (Fig. 2). The studied specimens average 93 x 60 mm with a 1.56 maximum length to width ratio (Table 1).

	Egg length (mm)	**Egg width (mm)**	**Length:width ratio**
Leipoa ocellata			
Mean	93.2	60.1	1.56
Median	93.8	60.7	1.55
Standard deviation	5.2	1.9	0.08
Range	86.9-101.8	56.8-62.5	1.39-1.70
N	16	16	16
Alectura lathami			
Mean	91.1	59.6	1.53

Median	91.2	70.0	1.53
Standard deviation	4.1	3.4	0.06
Range	82.2-98.9	53.8-70.0	1.4-1.6
N	22	22	22

Table 1: *Measurements of the eggs of* L. ocellata *and Alectura lathami. All specimens are curated at the Australian Museum*

Egg elongation allows for storing more nutrients, as the maximum egg diameter is constrained by the width of the pelvic opening of the hen. More nutrients facilitate a prolonged incubation and hyperprecociality, both typical aspects of megapode reproduction (Vleck et al., 1984; Booth, 1987b).

Figure 2:The 93 x 60 *elongated eggs of* L. ocellata *that differ from the typical galliform egg in shape and size. They are about three times the mass expected for galliform birds of this size. The extreme elongation is an adaptation to hyper precociality and the relatively thin eggshell an adaptation to lack of parental sit-on incubating strategy otherwise common to modern birds and a relatively long incubation period, 65-70 days for* L. ocellata*. The yellow squares measure 1x1 cm.*

Mallee fowl nest showing construction of varying mixtures of sand and organic material in a dry Australian environment.

Eggs of *L. ocellata* are deposited in a nest constructed in light soils, usually sand (Frith, 1956), where the partial pressure of oxygen is sub-atmospheric and that of carbon dioxide is higher than atmospheric (Seymour and Ackerman, 1980). The male constructs a mound mostly made of sand in open woodlands (Fig. 2) and tends the mound for up to 11 months per year (Frith, 1959). The same mound is often used in subsequent years (Frith, 1956; 1959) indicating a

nesting site fidelity, a nesting behavior similar tom that proposed for titanosaur nesting strategies (Grellet-Tinner et al., 2004, Grellet-Tinner et al., 2006; Hechenleitner et al., 2015). The egg chamber in the mound contains a core of decaying leaf litter covered by loose dry sand. The male opens the mound with his feet to expose the nest chamber of organic matter when the female approaches to oviposit. The female will not lay its eggs until she is satisfied with the excavation, presumably its temperature. Once the eggs are laid, the male covers them, then closes the mound, which results in all eggs being placed relatively centrally within a mound (Booth pers. communication). Temperatures in the mound range from 27-38 °C, although eggs are mostly exposed to 32-36°C (Booth, 1987a). Eggs can hatch at constant temperatures in the range of 32-38 °C, with an optimum of 34°C (Booth, 1987a). The incubation period depends on the temperature of incubation, varying from 45-50 days at 38 °C to 65-70 days at 32 °C (Booth, 1987b). In addition, female *L. ocellata* lay from 2-34 eggs in a season, depending on the food available in that season (Booth, 1987a). According to Vleck et al.(1984) and Booth (1987b) egg size varies considerably from 92-275 g, with means of 168, 173, and 187 g in different populations, and average 10.1-10.9% of the female weight (Marchant and Higgins, 1990). The long axis of the egg can lie in any orientation within the mound (Vleck et al., 1984). During incubation, approximately 21% of the inner surface of the eggshell is eroded, resulting in a three-fold increase in eggshell conductance (Booth and Seymour, 1987). The eggshell displays three structural layers (See Material and Method Section for eggshell structural components) that are overlaid by a relatively conspicuous external granular layer (Fig. 3). The total thickness of the eggshell averages 270 µm but varies from 258 to 280 µm associated with minor variables such as the preservation of the tips of mammillae cones and natural and/or man-made superficial erosion during the collection of the eggs. The eggshell surface appears nearly flat below the accessory layer, displaying just a weak undulation with scattered sparse and small nodes (Fig. 3). The inner three eggshell layers of *L. ocellata* are characteristic of the trilaminated structure (FSD and SEM

images) of most modern birds (Grellet-Tinner, 2006). Layer #1, the internal most structural eggshell layer, is formed by the mammillary cores and the calcite crystals that grow outward from the shell membranes during the shell formation (Fig. 5). This 105 µm layer is similar in thickness (within a few tenths of a micron) to layer #2 (FSD and SEM images), which is not common in modern eggs in which layer #2 is usually substantially thicker (Grellet-Tinner, 2006). The base of the shell units average 52 µm in width and are separated from each other by well-defined pore apertures that form a horizontal network parallel to and above the eggshell membranes (SEM images). Most of the pore canals that vertically transect the entire shell abut into this basal canal network. Layer #2 differs from layer #1 by its C-axis orientated in a different direction and irregular grain boundaries (Fig. 5). Layer 2 is characterized by short and bulky grains extending outward toward the external surface of the eggshell and a dominant calcite crystal orientation with a C-axis perpendicular to the outer surface. The boundaries between the grains in layer 2 are irregular (black lines in figure 5) with few small lateral offsets.

Layer 3 is quite obvious in SEM and FSD observations (Fig. 3). Its crystal orientation differs sufficiently from that of layer 2 (Fig. 3). Its thickness averages 57 µm, which is proportionally important for such a thin shell. The accessory layer appears delaminating from the eggshell structural layer #3 (Fig. 3C) and when observed in tangential view, the surface of this layer takes on the appearance of miniature mud cracks (Fig. 3D), both conditions potentially resulting from desiccation in the dry museum conditions.

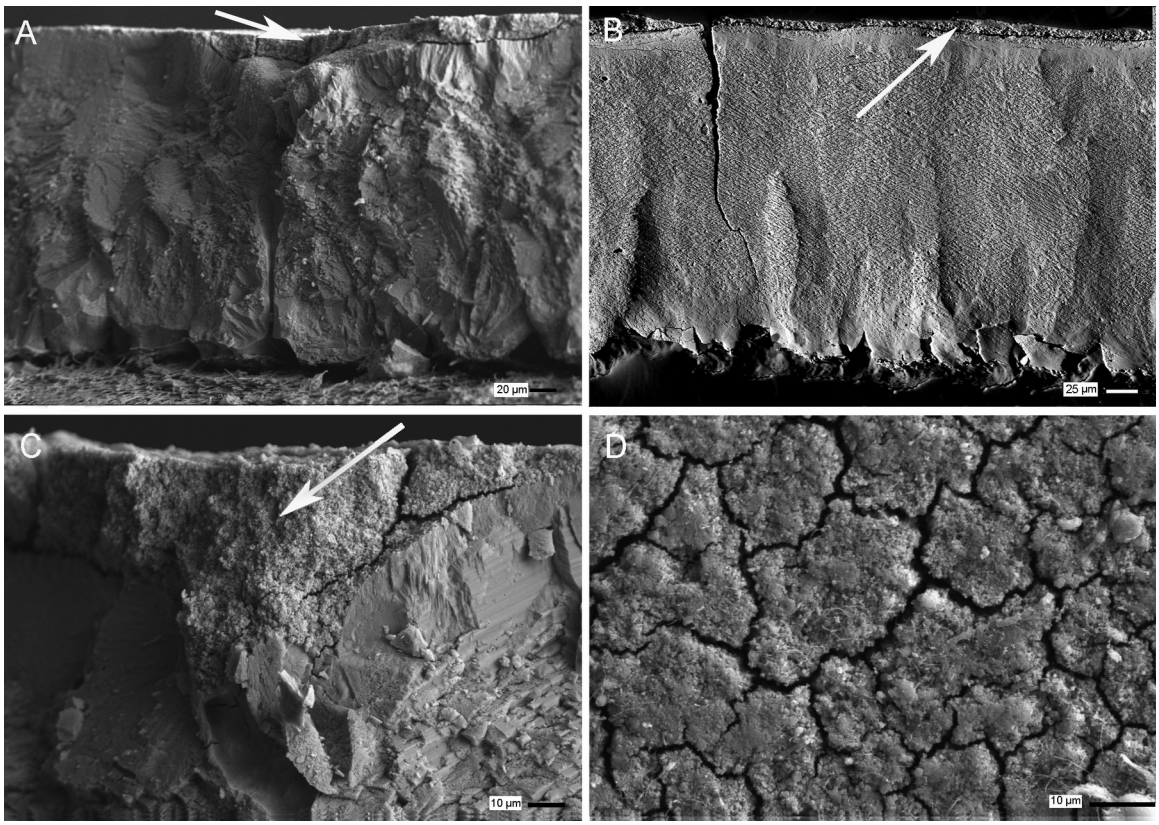

Figure 3: L. ocellata *SEMs. The eggshell displays three structural layers that are overlaid by a relatively conspicuous accessory granular layer (A, B, and C). The 270 µm thick eggshell displays just a weak undulation with scattered sparse and small nodes (A and B) covered by the accessory layer. The 105 µm thick layer #1 is formed by the mammillary cores and the calcite crystals that grow outward from the shell membranes during the shell formation (A). Layer #2 is nearly as thick as layer 1. Well-defined pore canals vertically transect the entire shell (A, B). The 57 µm layer 3 is quite obvious (A and B) as its crystal orientation differs from that of layer 2. The accessory layer is thick (C) and when observed in tangential view, the surface of this layer takes on the appearance of miniature mud cracks (D). Arrows point to the accessory layer.*

While noticeable in SEM, BSEM views and EDS images, (Figs. 3 and 4) the accessory layer is not visible in EBSD due to its amorphous make up (Grellet-Tinner et al., 2015). Therefore, the term accessory (or cuticle) in contrast to structural layer is entirely justified. It is 14 µm at its thickest and covers the entire eggshell; hence it masks all the pore apertures, concealing their shapes, and relative surficial position. This accessory layer consists of nano-size spheres (Fig. 3C). SEM, EBSD and EDS microcharacterizations show a large concentration of phosphate (Fig. 4) and a lesser concentration of calcium than the rest of the eggshell (Fig. 4), indicating that the primary mineral component of this accessory layer is calcium phosphate, as previously suggested by Board et al. (1981). This accessory layer, previously reported by Board

et al. (1982) in *L. ocellata* and D'Alba et al. (2014) in *A. lathami*, has antimicrobial properties that prevent infection of the developing embryo in the wet nesting environment (D'Alba et al., 2014). Although, accessory layers are not rare in avian eggs, the clade Podicipedidae+Phoenicopteridae (Tullett et al., 1976; Board et al., 1984), in addition to the Guinea fowl (Board et al., 1982), possess the same chemical and crystallographic accessory layer as *L. ocellata*. However, dromornithids, *Crax mitu*, *Anseranas semipalmata*, *Cereopsis novaehollandiae*, and *Cygnus atratus* also possess an accessory layer of calcium phosphate, albeit with minor crystallographic differences (Grellet-Tinner et al., 2015) in contrast to other avian eggs with vaterite (Tullett et al., 1976) or a waxy covering (Thompson and Goldie, 1990).

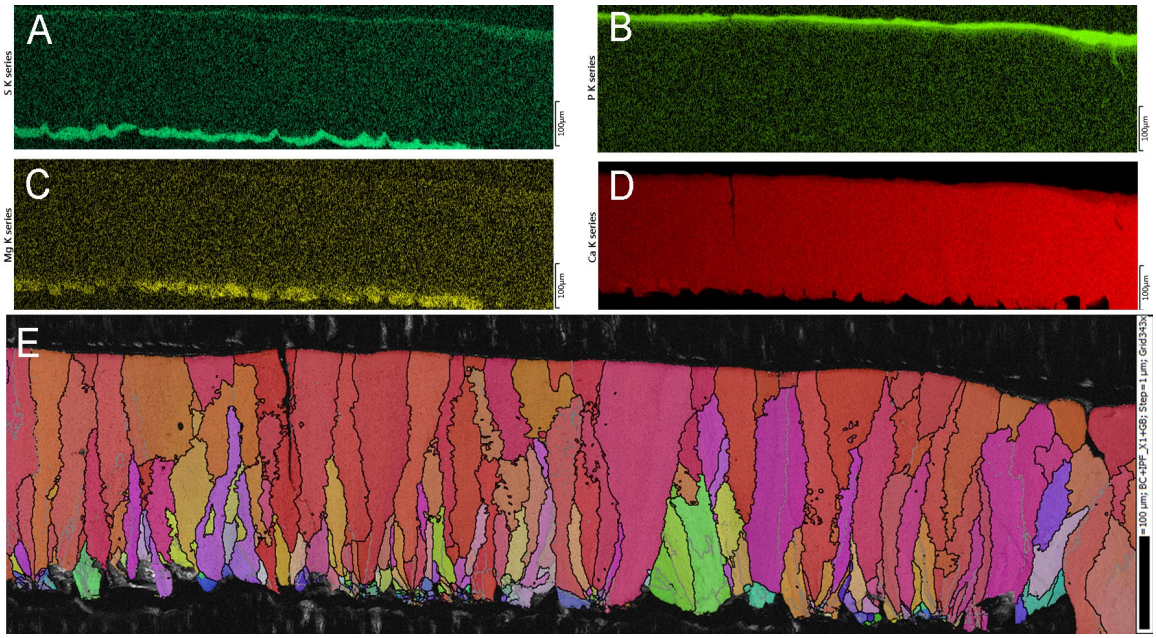

Figure 4:EDS and EBSD (See the orientation map in the M&M section) of the eggshell of L. ocellata. *Both microcharacterisations are performed at the same SEM instrument as indicated in M&M section. Sulfur (A) is present in the accessory layer and at the tip of the mammillae. The latter is congruent with the presence of the eggshell membranes. Phosphate (B) appears in substantial quantity in the AL. Magnesium(C) is present in both the AL and mammillae (also congruent with the presence of the eggshell membranes), Calcium (D) is the main component of the eggshell but shows a weak signal in the AL due to its large phosphate content. The EBSD (E) does not show the AL as it is not crystallized. Arrows point to the accessory layer.*

EDS analyses of the entire shell reveal small amounts of potassium (Fig. 4), and a large amount of magnesium (Fig. 4) in both the mammillae tips and moderately in the accessory layer, in contrast to Board et al., (1982), who identified only magnesium in the accessory layer of *L.*

ocellata. All Galliformes have magnesium in both regions in contrast to 60 bird species belonging to 19 Orders other than Galliformes (Board et al., 1982), where magnesium is only present in the mammillary cones (Board et al., 1982). Hence, the presence of Mg in both eggshell regions seems synapomorphic of Galliformes, excluding Anseriformes and megapodes (Board et al., 1982), which is not supported by our observations of megapodes. Interestingly, observations of flamingo eggshell also reveal the presence of magnesium in both locations, thus extending this character to phoenocopterids. Further EDS analysis located sulfur in both of these regions, which has never been reported for *L. ocellata*.

The spatial position of pore system in the eggshells is not readily observed using SEM or other classic microcharacterisations as they only offer a 2D resolution and pores may or may not be visible in a given surface regardless of the method used for observation. In addition, the pore apertures are masked by the accessory layer. Therefore, *L. ocellata* eggshells were micro scanned and the eggshell voids were digitally filled with blue pixels to define a 3D network. The rendering is of a 1.2 x 1.2 mm sample (Fig 5). Surface observations indicate 36 pore openings in this specimen, only 10 of which were distinct enough to render in 3D imaging. The rendering shows that the pores are paired, slit-like and located in minor depressions created by the weak nodular/undulatory surface of the shell. Each paired aperture opens to a canal that connects in layer 3, forming a Y shape that extends as a single tube nearly perpendicular to the eggshell surfaces down to the layers 2 and 3. This tube connects to a horizontal canal network parallel to, and above, the shell membranes. This network is formed by the depressions deeply excavated between the mammillae cones of layer 1. Interestingly, a similar network was previously reported in titanosaur eggshells (Grellet-Tinner et al., 2004; Grellet-Tinner 2005; Grellet-Tinner et al., 2012a, b, Hechenleitner et al., 2015).

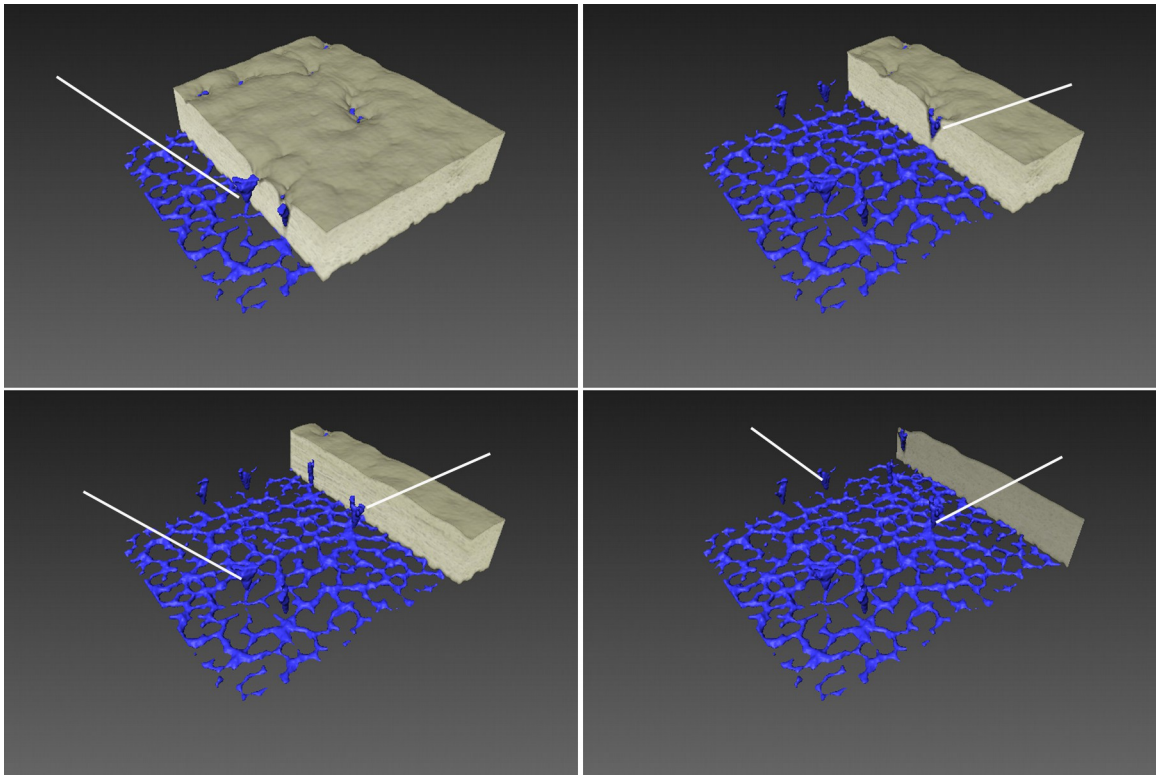

Figure 5: L. ocellata *micro-CT. The pores are paired, slit-like and located in minor depressions between the weak surficial nodes. Each paired aperture opens to canals that connect in layer 3, forming a Y (white arrows) shape that extends as a single tube nearly perpendicular to the eggshell surfaces. The tube connects to a horizontal canal network formed by the depressions deeply excavated between the mammillae cones above the eggshell membranes.*

Alectura lathami lays oval to pear shape eggs (Fig. 6), closer in shape to galliforms than those of *L. ocellata*, that are longer and more oval and elongate for nutrient storage to support prolonged incubation. The studied specimens measure 91 x 59.5 mm in linear dimension across the long and short axes of the egg with a 1.53 maximum length to width ratio (Table 1) chiefly in Queensland populations (Eiby and Booth, 2009), but are smaller in a South Australian population (Vleck et al., 1984). Nesting is timed to coincide with rainfall (summer in most of the range) (Frith, 1956). *Alectura. lathami* females lay from 18-24 eggs in a season, depending on the food available in that season (Jones et al., 1995). Estimates of clutch size in a mound vary considerably (Frith, 1956), presumably because eggs are laid and develop sequentially, rather than as an entire clutch. The eggs weigh 170-227 g (mean 202 g), representing 9% of the weight

of the female (Marchant and Higgins, 1990). Male *A. lathami* construct a mound consisting of dead leaf litter and topsoil (Fig. 6) each year in shaded forest areas (Frith, 1956).

Figure 6:Although 20% larger than L. ocellata*,* A. lathami *produces* 91 x 60 mm *eggs that are the same size than its congener. The eggs are relatively more proportionally shaped. They are incubated in 50-55 days by the heat generated from microbial activities in the mound. The yellow squares measure 1x1 cm.*
Male Alectura lathami *build a nest in forest undergrowth using topsoil and a variety of vegetal matter in the wet eastern Australian coastal region*

The male scrapes topsoil and vegetation adding to the mound throughout the nesting period, and occasionally turns over and mixes the upper layers of the nesting material (Frith, 1956; 1959). Females burrow into the mound vertically, but more often obliquely, by removing relatively less of the mound material in the process than *L. ocellata*. The litter material does not collapse around the tunnel as sand would in a mallee fowl mound (Booth pers. communication). Once the female is satisfied with the temperature at the end of her (typically 0.6-0.8 m long) tunnel, she lays her egg, and then does a "stampy dance" to initiate the tunnel back filling process, which is often interrupted by the male in attendance, which chases her away. The male then finishes repairing and adjusting the mound with the displaced nesting material. Hence, eggs can be located all over the place in large mounds but not just in the central core as in mallee fowl mounds (Booth pers. communication). The same egg grouping and dispersed variation have been observed in several titanosaur nesting sites (Hechenleitner et al., 2016). Nest temperatures average 34 °C, but egg temperatures can range from 24.5 to 40.7 °C (Eiby and Booth, 2008), exposing the eggs to wide

temperature fluctuations during incubation, without compromising incubation success (Eiby and Booth, 2008; 2009). Heavy rain results in reduced nest temperatures (Eiby and Booth, 2008). Eggs take six days longer to hatch at 32 °C (51.4 ± 0.4 days) than at 36 °C (45.6 ± 0.9 days), which influences the mass of hatchlings, with larger hatchling emerging from eggs incubated at warmer temperatures (Eiby and Booth, 2009).

The eggshell displays three structural layers overlaid by a relatively conspicuous external granular layer (Fig. 7) that is extremely thick above troughs created between the nodes on the surface. Unlike *L. ocellata*, the outer surface of the shell of *A. lathami* has a pronounced nodular ornamentation (Fig. 9), a feature not previously reported. Observations of randomly selected polar and equatorial sections do not present noticeable differences in nodular size or concentration. The nodes are densely packed, mirroring in some respect those of extinct nemegtosaurid titanosaurs (Grellet-Tinner, 2005; Grellet-Tinner et al., 2012a; Hechenleitner et al., 2015) from Hateg in Transylvania and AM L#4. Another distinctive feature of the microstructure of the eggshell of *A. lathami* is its porosity, expressed by an abundance of pore canals visible in SEM imaging (Fig. 7). The pores extend from funnel-shaped apertures between each node and interconnect at several levels of the eggshell, thus forming a multidimensional network. This feature also mirrors that of extinct nemegtosaurid titanosaurs (Grellet-Tinner, 2005; Grellet-Tinner et al., 2012a).

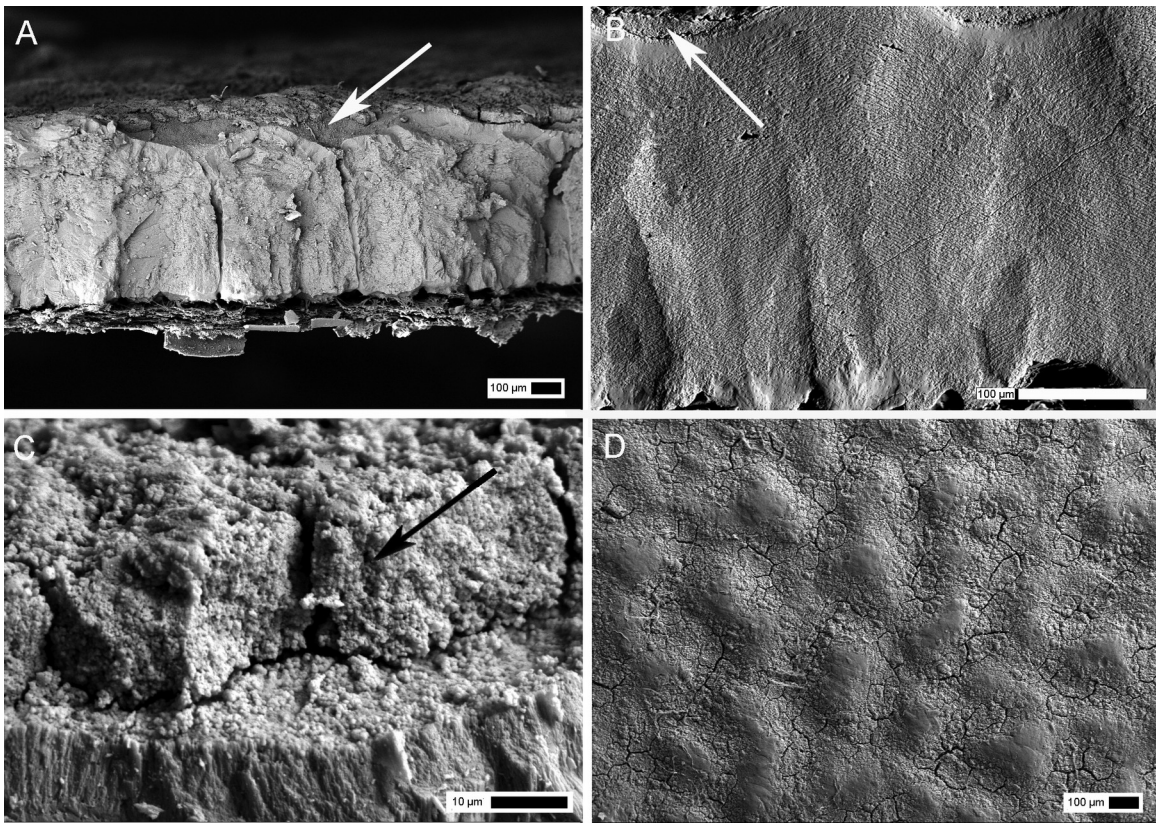

278 *Figure 7:* A. lathami *SEMs. The eggshell displays three structural layers that are overlaid by a*
279 *relatively conspicuous accessory granular layer (A, B, and C). The 353 µm eggshell displays*
280 *three structural layers overlaid by a relatively conspicuous external granular layer like* L.
281 ocellata *but unique to modern birds its outer surface displays a pronounced nodular*
282 *ornamentation (A, B, an D), mirroring in some respect that of extinct nemegtosaurid titanosaurs.*
283 *The eggshell porosity is high expressed by a notable abundance of pore canals (A). Arrows point*
284 *to the accessory layer.*

285 The total thickness of the eggshell averages 353 µm but varies from 348 to 359 µm
286 because of the height differences among the nodes. The trilaminated structure (Fig. 7A) in *A.*
287 *lathami* is characteristic of most modern avian eggshells (Grellet-Tinner, 2006). Layer #1 is
288 formed by the mammillary cores and the calcite crystals that grow outward from the shell
289 membranes during the shell formation (Fig. 7A,B). However, these crystals do not radiate as
290 much in a semi-circular pattern, nor are they as slender as those of *L. ocellata* (Figs. 3 and 97B).
291 They appear wider and flatter at their base, up to 95 µm in width. This innermost layer is
292 extremely thick, reaching 209 µm, which greatly exceeds that of *L. ocellata*. It accounts for most
293 of the eggshell thickness, which is not common in modern eggs in which layer #2 is usually

294 substantially thicker (Grellet-Tinner, 2006). Like *L. ocellata*, the base of the shell units are
295 separated from each other by well-defined pore apertures that form a horizontal network parallel
296 to and above the shell membranes (Fig. 7). The 100 µm layer 2 is relatively and disproportionally
297 thin for an extant bird. Layer #2 differs from layer #1 by its C-axis orientated in a different
298 direction and irregular grain boundaries (Fig. 10), but aligned with those of Layer 3. As such,
299 layer 3 is not distinct from layer 2 in EBSD, although noticeable in SEM characterizations. Its
300 thickness does not exceed 37 µm, which is proportionally important for such a thin shell, but it is
301 thinner than in the eggs of *L. ocellata.* The accessory layer appears delaminating from the
302 eggshell structural layer #3 (Fig. 7) and, when observed in tangential view, the surface of this
303 layer looks like miniature mud cracks (Fig. 7D), potentially resulting from desiccation in the dry
304 museum conditions. While noticeable in SEM, BSEM views and EDS images, the accessory
305 layer (Fig. 8) is not visible in EBSD due to its amorphous make up. It is 23 µm thick over a node
306 but reaches 75 µm at its thickest when it covers the pore apertures lodged deep in between the
307 nodes. The accessory layer consists of nanospheres (Fig. 7C). Like *L. ocellata* SEM, the primary
308 mineral component of the accessory layer is calcium phosphate (Fig. 8). EDS analyses of the
309 entire shell reveal a large amount of magnesium and sulfur (Fig. 8) in the mammillae tips, with
310 less in the accessory layer. Silicate appears as a moderate signal only in the accessory layer,
311 which is unusual as the eggs were collected fresh and blown for collection purposes. Although
312 the most parsimonious origin of this silicate should be by contamination of the nesting material,
313 its presence within the fabric of the accessory layer is bewildering and could indicate a biological
314 origin.

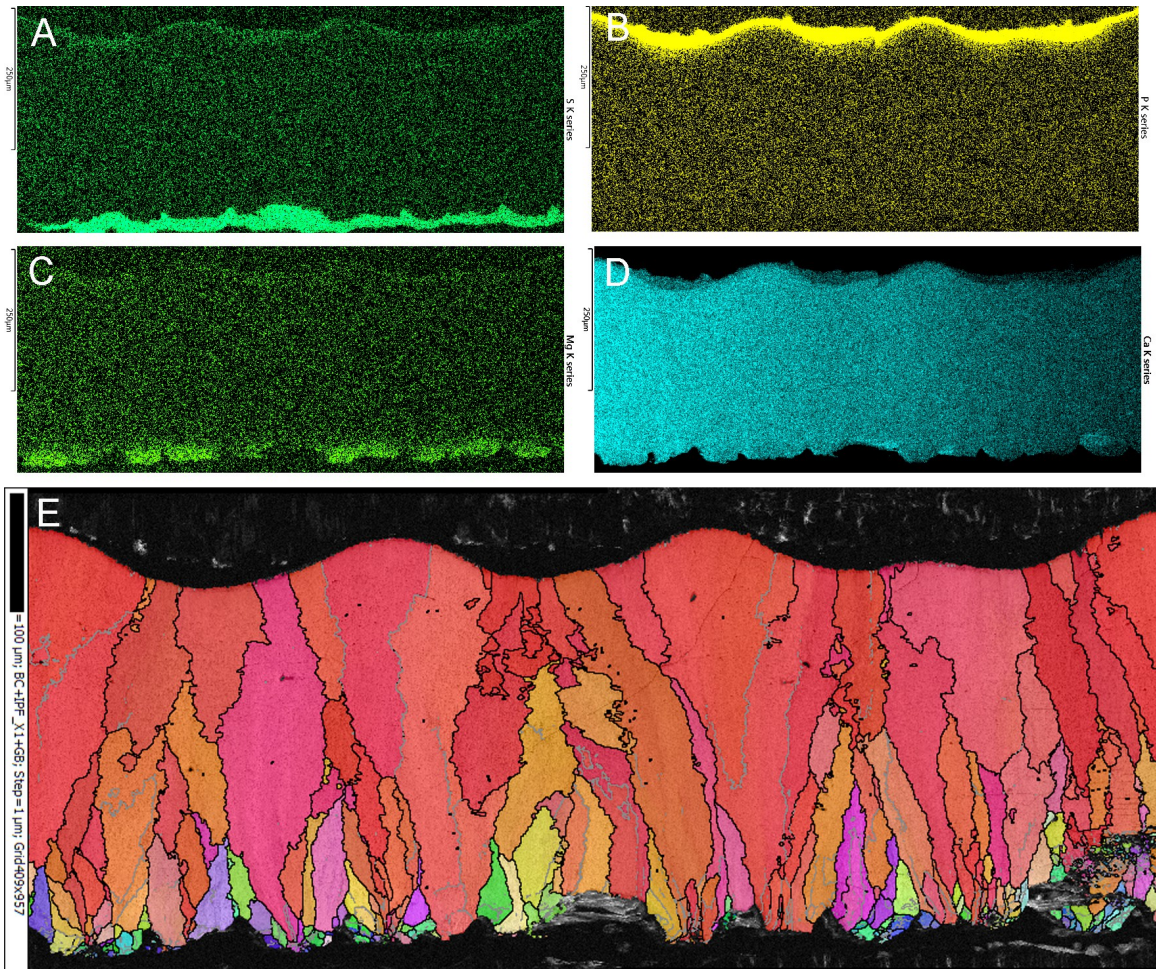

Figure 8: A. lathami *EDS and EBSD (See the orientation map in the M&M section). Sulfur (A) is present in the accessory layer and at the tip of the mammillae. The latter is congruent with the presence of the eggshell membranes. Phosphate (B) appears in substantial quantity in the AL. Magnesium(C) is present in both the AL and mammillae (also congruent with the presence of the eggshell membranes), Calcium (D) is the main component of the eggshell but shows a weak signal in the AL due to its large phosphate content. The EBSD (E) does not show the AL as it is not crystallized. Note the ubiquitous nodes in both EDS and EBSD microcharacterisations. Arrows point to the accessory layer.*

The pore apertures and canals are obvious in SEM images, but their network is only fully revealed using 3D imaging from micro-CT rendering (Fig. 9). Surface observations of the micro –CT sample indicate more than 25 nodes on this 1.2 x 1.2 mm specimen, where 2 or 3 of them coalescent into a single longer feature. The pore openings are nested in the depressions between adjacent nodes. Only 7 pores had enough contrast to be rendered in 3D imaging. Pore apertures separated only by 1 node have a tendency to have their canals connecting at the limit of layer 3

329 and 2, forming a distinct Y shape (Fig. 9), reminiscent of those observed in nemegtosaurid
330 titanosaurs from the Cretaceous Hateg Island (Grellet-Tinner et al., 2012a, b) and AM L #4
331 (Grellet-Tinner, 2005; Hechenleitner et al., 2015). In addition to this branching, the Y-shaped
332 pore canals connect laterally to each other in the mid-section of layer 1 (Fig. 9), creating a
333 horizontal network parallel to the shell inner surface. A very conservative estimate of 3
334 horizontal connections in 1.44 mm2, suggests 1513 horizontal connections in the whole
335 egg, The lower trunks of these joined canals abut to a horizontal canal network parallel to, and
336 above, the shell membranes, similarly to *L. ocellata*. This network is formed by the deep

depressions between the mammillae cones of layer 1.

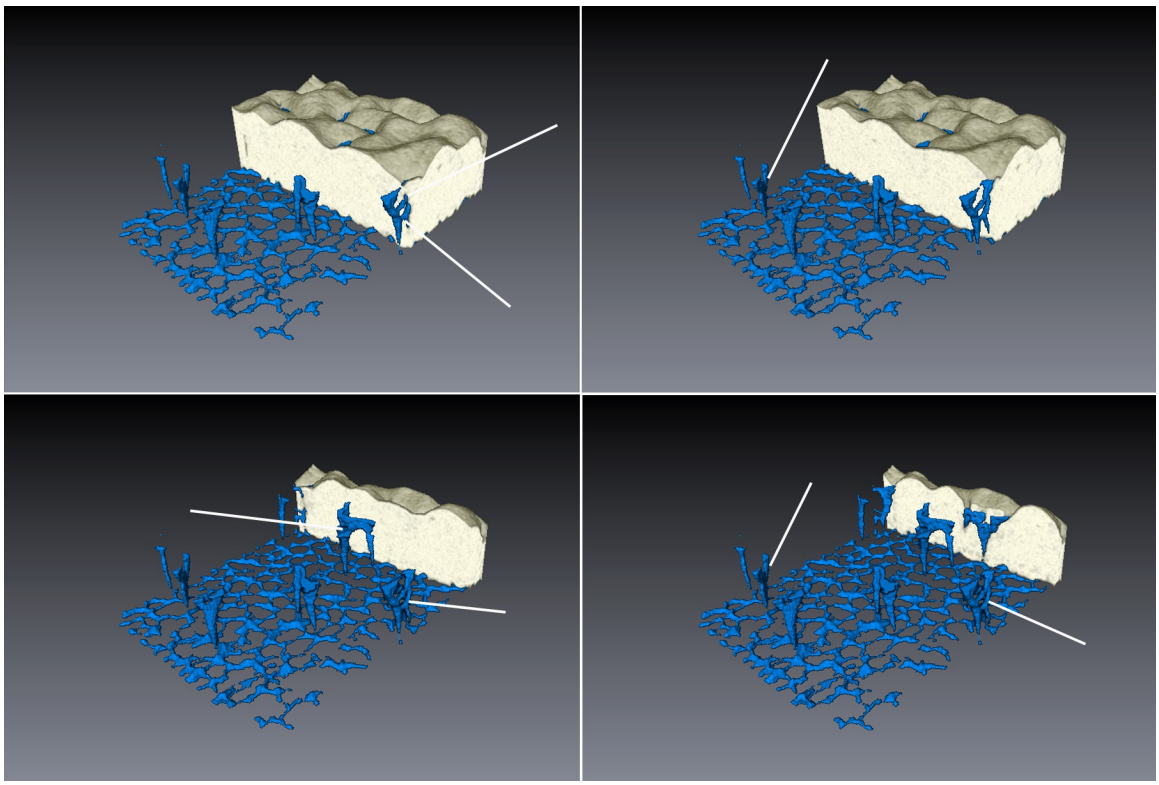

*Figure 9:*A. lathami micro-CT. *The pore apertures of are located in depressions between nodes lead to canals in blue that connect forming a distinct Y shape (white arrows). They connect laterally to each other in the mid-section of layer 1, creating a horizontal network (white arrows) parallel to the shell inner surface. Such pore networks have been observed in titanosaur dinosaurs, but not in any extant bird.*

Discussion

The eggs of both species are oviposited in egg chambers inside incubating mounds and are yolk-rich producing highly precocial hatchlings (Vleck et al., 1984; Eiby and Booth, 2009). The egg chambers have high relative humidities and, although the eggs lose some water during incubation, the loss is less than in species that have open nests (Seymour et al., 1987; Eiby and Booth, 2009). Although both species are mound builders, there are some striking differences in their nesting behaviours, eggs, and eggshells. *Leipoa ocellata* is 20% smaller than *A. lathami*, but produces eggs that are the same size (Vleck et al., 1984), but eggs of *A. lathami* have a thicker eggshell, regardless of the inclusion of surface nodes in the thickness measurement. This raises two interesting questions of why a smaller species would lay proportionally larger eggs and why the smaller eggs of the other species have a thicker and nodular eggshell? The fact that the smaller species lays proportionally larger eggs is most likely related to a minimum egg size or volume needed for sustaining an extended incubation: 65-70 days for mallee fowl (Booth, 1987b) and to 51 days in brush turkeys (Eiby and Booth, 2009) at 32 °C, compared to 21 days for chicken eggs. Regardless, both species lay eggs that are 3 times that of a galliform (S1) of similar body weight (Rahn et al., 1975), because of their extreme precociality and relatively long incubation period (Vleck et al., 1984). These large weight disparities are explained by the unique incubation strategies utilizing environmental heat, where eggs hatch after 50 days of incubation in their natural environment and the hatchlings show extreme precociality, like those of titanosaurs (Curry Rogers et al., 2016).

As these two Australian mound builders do not live in the same environments, their nests differ in size and in their building material. Nonetheless, the eggshells of both species possess calcium phosphate in the form of nanospheres that create a thick accessory layer. The super-hydrophobicity and high contact-angle-hysteresis properties of this layer have been well

documented (D'Alba et al., 2014). Water droplets remain pinned to the surface and thus do not roll off but trap condensed water at discrete points, preventing it from spreading uniformly over the surface and thereby inhibiting biofilm formation that could block pores, which could compromise oxygen uptake by the embryo. *Alectura lathami* thrives in moist coastal environments and does not extend to the semiarid environments inhabited by *L. ocellata* and their nests contain more vegetal matter than those of *L. ocellata*. The incubating heat in these compost-mounds is produced by microbial decomposition of organic matter (Jones, 1988), which results in an increase of organic acids. Although 1.5 times thinner than chicken eggshells, at 353 µm the eggshell of *A. lathami* greatly exceeds the 270 µm thickness of *L. ocellata* eggshells. This greater thickness, coupled with a large number of nodes in *A. lathami*, is here hypothesized as an adaptation to an environment rich in organic acids by avoiding any outer shell chemical thinning at the early stage of embryonic development. Similar compensation for potential chemical erosion has also been reported for neosauropod dinosaurs (Grellet-Tinner and Fiorelli, 2010, Hechenleitner et al., 2015, 2016). The nodes are initially the only shell structures in direct contact with the nesting material, hence they could be eroded by chemical leaching leaving the eggshell thickness intact, thus allowing for diffusion of respiratory gases during the extended incubation time. This hypothesis is supported by the reported thinning of the external surfaces of eggshells in titanosaur nesting sites (Grellet-Tinner and Fiorelli, 2010, Hechenleitner et al., 2015, 2016). Moreover, we suggest the internodal spaces act as funnels which, together with the accessory layer, concentrates condensed water vapor where, for the megapodes, the greater thickness of calcium phosphate nanospheres is located (above the pore apertures located between the nodes). Concomitantly, this water funneling may reduce the likelihood of bacterial infection, as the thicker calcium phosphate creates a greater microbial barrier. The presence of very small nodes in *L. ocellata* supports this hypothesis, as its mound is mostly sandy, thus with less organic acids than *A. lathami*. These megapode eggshell autopomorphies and adaptations to two different

environments and climates mirror those observed in the Auca Mahuevo (AM) titanosaur nesting site (Hechenleitner et al., 2015), where the egg-laying titanosaurs in AM L#4 may represent a different nemegtosaurid species, certainly closely related to those nesting in AM layers 1-3 (AM L#1-3) but displaying sufficient autapomorphies to justify a species variation (Eagle et al. 2015). This species variation has been further supported by an environmental change supported by several geological observations (Hechenleitner et al., 2015). In addition, geochemical analyses reveal a high concentration of magnesium and lithium in AM L#1-3 than AM L#4 (Eagle et al., 2015). The evidence available suggests Auca Mahuevo has been selected first by a certain nemegtosaurid species (AM L#1-3) for its presence of limited rivers in a semiarid environment (Grellet-Tinner, Chiappe & Coria, 2004; Grellet-Tinner et al., 2012) and then, after a climatic change toward wetter conditions, replaced by another closely related species with more conspicuous nodular eggshell ornamentation (AM L#4), adapted to a more humid nesting environment (Hechenleitner et al., 2015), and with eggshell ornamentations and pore structures that mirror those of *A. lathami*. Although both megapode species are contemporaneous, unlike the two species of titanosaurs at the Auca Mahuevo nesting site, their geographic distribution is related to vegetation and climatic differences. Such species-specific nesting partitioning in modern Australia may explain the successive nemegtosaurid species replacement in Auca Mahuevo from a dryer environment nesting adaptation, such as occurs in AM L#1-3, to a wetter setting, recorded upwards by the transition to the Allen Formation (Hechenleitner et al., 2015).

The y-shaped pores in the eggshells of both species (Figs. 5 and 9) are well known in megapodes (Booth and Thompson, 1991), but the single or double horizontal connections between adjacent pores in *A. lathami* (Fig. 9) have not been observed previously. Although occurring only three times in the 1.2mmx 1.2 mm micro scanned sample, these horizontal pore connections must be common given the small size of the specimen and the partial rendering of all the pore canals in this sample. Although the function of these connections is not known in

modern birds, it has been observed in the eggs from the AM L#4 and the Cretaceous titanosaur nesting sites in Transylvania where the dinosaurs nested in extremely wet environments (Grellet-Tinner and Fiorelli 2010; Grellet-Tinner et al., 2012a). Based on present observations, the horizontal connections would facilitate the lateral diffusion of respiratory gases in the event of occlusion of pores on the surface of the egg.

The accessory layer of both megapode species possesses sulfur, which is not present in the eggshells of other galliforms, but occurs in flamingo eggs. Sulfur in the accessory layer of megapodes has never been reported, and hence its function has not been investigated. Considering the well-known antibacterial and anti-fungal properties of organic sulfur in its various states, we propose that its presence in the accessory layer of mound-builder megapode provides a complementary barrier to the calcium phosphate nanospheres for bacterial and fungal contamination, which is entirely consistent with its occurrence in flamingo eggs. Independently, the phosphate content in the accessory layer may delay the acidification and dissolution of the calcium carbonate shell as exposed to organic acids, thus adding another function to this layer in the evolutionary adaptation of these two megapode species to mount-nesting strategies.

Material and methods

The blown eggs of *A. lathami* and *L. ocellata* used for this study are curated at the Australian Museum in Sydney (Table 1). Each egg was photographed with minimal parallax and measured with digital calipers.

SEM of whole mount eggshells was performed at the Australian Museum Scanning Electron Microscope Facility. The specimens were mounted on aluminum stubs via carbon conductive glue and carbon tabs. The stubs were gold sputter coated using an Emitech K550 coater. The samples were examined under the Zeiss Evo LS15 SEM using both the Robinson

Backscatter detector and the Everhart-Thornley SE detectors following Grellet-Tinner (2006) protocol.

EBSD microcharacterisations were performed at the University of Sydney ACMM. EBSD and EDS analyses were carried out using a Zeiss Ultra Plus field emission gun SEM, equipped with an Oxford Instruments AZtec microanalysis system, including an X-Max 20 silicon drift EDS detector and a Nordlys Nano EBSD detector.

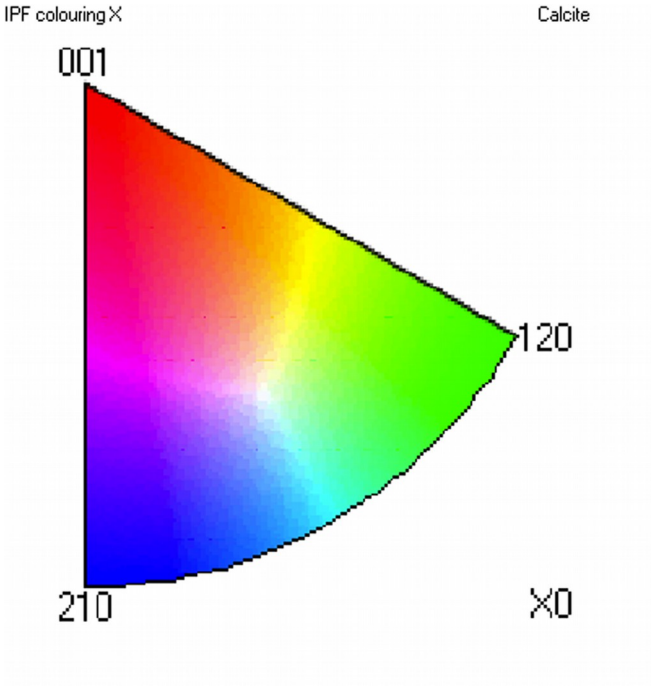

The colours show the calcite crystal direction that is parallel to shell normal direction. Red colours indicate that the c-axis is normal to the shell surface, whereas green and blue colours show that the c-axis lies within the shell plane, with a- or m- axes aligned normal to the shell surface.
The beam energy was set to 20 kV, with a beam current of 2-5 nA. EBSD data were further processed using Oxford Instruments CHANNEL5 software. Prior to microstructural analysis at the SEM, samples were polished down to 1µm diamond paste (Trimby and Grellet-Tinner, 2011) and finished with 3-5 minutes of polishing using colloida silica suspension (Struers OPS). The samples were then coated with approximately 5 nm of carbon to remove charging.

Micro-CT microcharacterisations were performed at the University of Sydney ACMM. The eggshell specimens were scanned using an Xradia MicroXCT-400 system operating at 55-60

keV and 127-133 mA. The specimens were mounted in low-density polystyrene to prevent movement during their 360 ° rotation with projections collected at 0.2 ° intervals. System geometry and objective lenses were used to scan at a pixel resolution of 4.6 and 19 µm for *L. ocellata and A. lathami* respectively. Image stacks were rendered using Avizo Fire (VSG|FEI Visualization Sciences Group) as well as the internal pore networks labelled using thresholding techniques. Pore volume calculations were obtained by running a material calculation on the samples with each voxel being assigned to one of pore, shell or exterior (air) based on grey level/x-ray absorption.

Observations of two polar and one equatorial sections of an *A. lathami* egg (A915-16-18a) were performed to test if there were any eggshell structural variations in an egg.

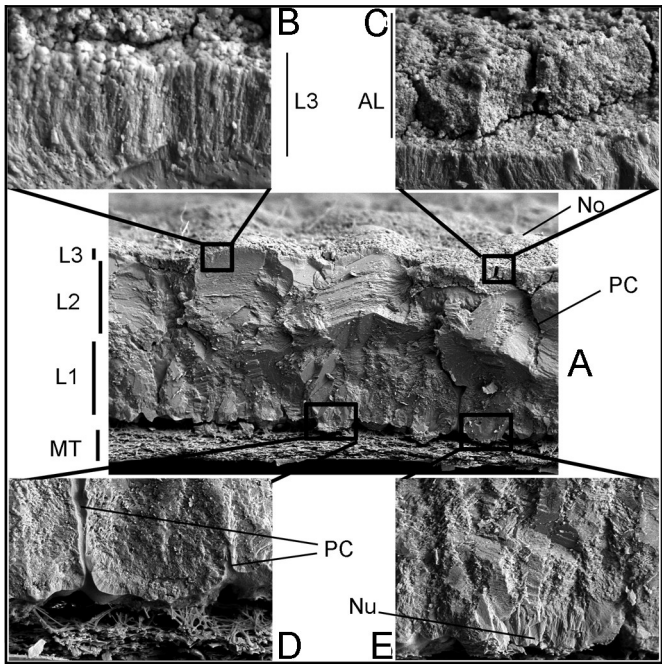

Eggshell structural components: A: SEM of a radial section of an eggshell of *Alectura lathami* (Australian brush turkey specimen) that belongs to an egg in which the embryo had not developed or was infertile.
B: High magnification SEM of the contact between layer 3 and the accessory layer. Note the elongated calcite crystals of layer 3.
C: High magnification SEM of the contact between the accessory layer and L3. Note the spherule shape of the amorphous calcite in the accessory layer that blankets layer 3.
D: High magnification SEM of the base of the eggshell. Note the organic filaments of the eggshell membranes that are embedded at the base of the calcitic eggshell units and the pore canals that each abuts in cavities formed between the eggshell units in not-incubated egg.

E: High magnification SEM of the base of the eggshell units. Note the radiating calcite crystals that grow outward to form the eggshell units.
L1: layer 1
L2: layer 2
L3: layer 3
AL: Accessory layer
MT: Membrana testacea (eggshell membranes)
PC: Pore canal
No: Surface node
Nu: Eggshell nucleus

487 **Table**

	Egg length (mm)	Egg width (mm)	Length:width ratio
Leipoa ocellata			
Mean	93.2	60.1	1.56
Median	93.8	60.7	1.55
Standard deviation	5.2	1.9	0.08
Range	86.9-101.8	56.8-62.5	1.39-1.70
N	16	16	16
Alectura lathami			
Mean	91.1	59.6	1.53
Median	91.2	70.0	1.53
Standard deviation	4.1	3.4	0.06
Range	82.2-98.9	53.8-70.0	1.4-1.6
N	22	22	22

488 **Supplementary data**

489 From Rahn et al., 1975 Auk 92:750-765.

490 Common regression equation for the 17 orders of birds:

491 $W = 0.277\ B^{0.770}$

492 where W = egg mass in g, and B is bird body mass in g.

493 We think that the exponent has a typo in it and it should be 0.670. When I calculate the mean of

494 the exponent values given in Fig. 1 for each of the Orders of birds and families of passerines, we

495 obtain 0.682.

496 Using $W = 0.277\ B^{0.770}$ the predicted egg weight for a 2.5 kg brush turkey would be 114.5 g

497 (range for 2.1-2.9 kg would be 100.1-128.4 g) compared to a published mean of 202 gm and for a

498 1.8 kg mallee fowl it would be 88.9 gm (range for 1.5-2.0 kg would be 77.3-96.4 g), compared to

499 published means of 168, 173 and 187 gm)

500 Using what should be the correct equation $W = 0.277\ B^{0.670}$

The predicted egg weight for a 2.5 kg brush turkey would be 52.4 g (range for 2.1-2.9 kg would be 46.6-56.5 g) compared to a published mean of 202 gm.and for a 1.8 kg mallee fowl it would be 42.0 gm (range for 1.5-2.0 kg would be 37.2-45.1 g), compared to published means of 168, 173 and 187 gm)

But in Figure 1 of Rahn et al. (which is really a table), the equation for Galliformes is:

$W = 0.484\ B^{0.640}$

Bird mass	Species	Real egg mass	$W = 0.277\ B^{0.770}$	$W = 0.277\ B^{0.670}$	$W = 0.484\ B^{0.640}$
			Equation for all birds (may be incorrect)	Assumed correct equation for all birds	Equation for galliformes
1.5	MF (small)	168, 173, 187	77.3	37.2	52.2
1.8	MF (~mode)	168, 173, 187	88.9	42.0	58.6
2.0	MF (large)	168, 173, 187	96.4	45.1	62.7
2.1	BT (small)	202	101.1	46.6	64.7
2.5	BT (~mode)	202	114.5	52.4	72.4
2.9	BT (large)	202	128.4	56.5	79.6

Acknowledgements

The work was conducted as part of a University of Sydney Research Collaboration Award to GGT, and support from the University of Sydney to MBT and NSF/1329471to GGT. The project was made possible through the assistance of the Australian Museum, especially J. Sladek, R. Sadlier, L. Tsang, and W. Boles. The Australian Centre for Microscopy and Microanalysis, especially P. Trimby and M. Foley was instrumental for the microcharacterisations of the studied specimens. Ideas in this paper were developed in part through discussions with, G. Prideaux, T. Worthy, R.S. Seymour, and D.T. Booth. We thank Jacqueline Herbert for her help formatting the manuscript.

Statement of financial and non-financial competing interests

We declare no financial competitive interests for any authors of this manuscript.

References

Birks SM, Edwards SV. 2002. A phylogeny of the megapodes (Aves: Megapodiidae) based on nuclear and mitochondrial DNA sequences. Molecular Phylogenetics & Evolution 23:408-421. doi:10.1016/S1055-7903(02)00002-7

Board RG, Perrott G, Love G, Seymour RS. 1982. A novel pore system in the eggshells of Mallee Fowl *Leipoa ocellata*. Journal of Experimental Zoology 220:131-143. doi: 10.1002/jez.1402200118

Board R, Perrott H, Love G, Scott V. 1984. The phosphate-rich cover on the eggshells of grebes (Aves: Podicipitiformes). Journal of Zoology 203:329-343. doi: 10.1111/j.1469-7998.1984.tb02336.x

Boles W, Ivison T. 1999. A new genus of dwarf Megapode (Galliformes: Megapodiidae) from the late Oligocene of central Australia. In: Olson SL (eds). Avian Paleontology at the Close of the 20th Century: Proceedings of the 4th International Meeting of the Society of Avian Paleontology and Evolution, Washington, DC, Smithsonian DOI: 10.5479/si.00810266.89.1

Booth DT. 1987a. Home range and hatching success of Malleefowl, *Leipoa ocellata* Gould (Megapodiidae), in Murray mallee near Renmark, SA. Australian Wildlife Research 14:95-104. doi:10.1071/WR9870095

Booth DT. 1987b. Effect of temperature on development of Mallee Fowl *Leipoa ocellata* eggs. Physiological Zoology 60: 437-445. Stable URL: http://www.jstor.org/stable/30157905

Booth DT, Seymour RS. 1987. Effect of eggshell thinning on water-vapor conductance of Malleefowl eggs. Condor 89:453-459. doi:10.2307/1368635

Booth DT, Thompson MB. 1991. A comparison of reptilian eggs with those of megapode birds. In: Deeming DC, Ferguson MWJ. (eds). Egg Incubation: Its Effect

on Embryonic Development in Birds and Reptiles. Cambridge University Press. pp. 325 344.

Curry Rogers K, Whitney M, D'Emic M, and Bagley B. 2016. Precocity in a tiny titanosaur from the Cretaceous of Madagascar. Science; 352(6284): 450-3.

D'Alba L, Jones DN, Badawy HT, Eliason CM, Shawkey MD. 2014. Antimicrobial properties of a nanostructured eggshell from a compost-nesting bird. The Journal of Experimental Biology 217: 1116-1121. doi:10.1242/jeb.098343

Dekker RWRJ, Brom TG. 1992. Proceedings of the First International Megapode Symposium, Christchurch, N. Z., Dec. 1990

Del Hoyo J, Elliot A, Sargatal J. 1994. Handbook of the Birds of the World, Vol 2: New World Vultures to Guinea Fowl. 638 pp. Barcelona: Lynx Editions.

Eagle RA, Enriquez M. Grellet-Tinner G, Pérez-Huerta A, Hu D, Tütken T, Montanari S, Loyd SJ, Ramirez P, Tripati AK, Cerling TE, Chiappe LM, and Eiler JM. 2015. Isotopic (^{13}C-^{18}O) ordering in calcium carbonate eggshells reflects body temperatures and suggests differing thermophysiology in two Cretaceous dinosaurs**.** Nature Communications. http://www.nature.com/ncomms/2015/151013/ncomms9296/full/ncomms9296.html.

Eiby YA, Booth DT. 2008. Embryonic thermal tolerance and temperature variation in mound of the Australian Brush-turkey (*Alectura lathami*). Auk 125:594-599. doi:10.1525/auk.2008.07083

Eiby YA, Booth DT. 2009. The effects of incubation temperature on the morphology and composition of Australian Brush-turkey (*Alectura lathami*) chicks. Journal of Comparative Physiology B 179:875-882. doi:10.1007/s00360-009-0370-4

Frith HJ. 1956. Breeding habits of the family Megapodiidae. Ibis 98:620-640. doi:10.1111/j.1474-919X.1956.tb01453.x

Frith HJ. 1959. Breeding of the mallee fowl *Leipoa ocellata* Gould (Megopodiidae). C.S.I.R.O.

Wildlife Research 4:31-60. doi: 10.1071/cwr9590031

Göth A, Vogel U 1997. Egg laying and incubation of the Polynesian megapode. Annual Review World Pheasant Association 1996/97:43–54.

Grellet-Tinner G. 2005. The membrana testacea of titanosaurid dinosaur eggs from Auca Mahuevo (Argentina): Implications for the exceptional preservation of soft tissue in Lagerstätten. Journal of Vertebrate Paleontology 25:99-106. doi:10.1671/0272-4634(2005)025[0099:mtotde]2.0.co;2

Grellet-Tinner G. 2006. Phylogenetic interpretation of eggs and eggshells: implications for oology and Paleognathae phylogeny. Alcheringa 30:130-180. doi:10.1080/03115510608619350

Grellet-Tinner G, Chiappe L, Coria R. 2004. Eggs of titanosaurid sauropods from the Upper Cretaceous of Auca Mahuevo (Argentina). Canadian Journal of Earth Sciences 41:949–960. doi:10.1139/e04-049

Grellet-Tinner G, Fiorelli L. 2010. A new Argentinean nesting site showing neosauropod dinosaur reproduction in a Cretaceous hydrothermal environment. Nature Communications 1:1-8. doi:10.1038/ncomms1031

Grellet-Tinner G, Codrea V, Folie A, Higa A, Smith T. 2012a. First evidence of reproductive adaptation to “Island effect” of a dwarf Cretaceous Romanian titanosaur, with embryonic integument in ovo. Plos One 7:e32051. doi:10.1371/journal.pone.0032051

Grellet-Tinner G, Fiorelli L, Salvador R. 2012b. Water vapor conductance of the lower Cretaceous dinosaurian eggs from Sanagasta, La Rioja, Argentina: Paleobiological and paleoecological implications for South American faveoloolithid and megaloolithid eggs. Palaios. DOI: 10.2110/palo.2011.p11-061r.

590 Grellet-Tinner G, Spooner NA, and, Worthy TH. 2016. Is the "Genyornis" egg of a mihirung or
591 another extinct bird from the Australian dreamtime? Quaternary Science Reviews, 133:147-164.
592 DOI: 10.1016/j.quascirev.2015.12.011.

593 Harris R, Birks SM, Leache AD. 2014. Incubator birds: Biogeographical origins and evolution of
594 underground nesting in megapodes (Galliformes: Megapodiidae). Journal of Biogeography
595 41:2045–2056. doi:10.1111/jbi.12357

596 Hechenleitner ME., Grellet-Tinner G, Fiorelli. L. 2015. What do giant titanosaur dinosaurs and
597 modern Australasian megapodes have in common? *PeerJ*: PeerJ 3:e1341
598 https://dx.doi.org/10.7717/peerj.1341.

599 Hechenleitner EM**,** Grellet-Tinner G, Foley M, Fiorelli LE, Thompson MB. 2016 Micro-CT scan
600 reveals an unexpected high-volume and interconnected pore network in a Cretaceous Sanagasta
601 dinosaur eggshell. *Journal of the Royal Society. Interface* **13**: 20160008.

602 Jones DN. 1988. Construction and maintenances of the incubation mounds of the Australian
603 brush-turkey *Alectura lathami*. Emu 88:210-218. doi:10.1071/mu9880210

604 Jones DN, Dekker RWRJ, Roselaar, CS. 1995. The Megapodes: Oxford University Press. (6)
605 Sibley CG, Monroe BL Jr. 1990. Distribution and Taxonomy of Birds of the World. New Haven,
606 Yale University Press.

607 Marchant S, Higgins PJ (eds). 1990. Handbook of Australian, New Zealand and Antarctic Birds.
608 Volume 1: Ratites to Ducks. Oxford University Press, Melbourne

609 Paganelli CV. 1980. The physics of gas exchange across avian eggshell. American Zoologist
610 20:329-338. doi:10.1093/icb/20.2.329

611 Rahn H, Paganelli CV, Ar A. 1975. Relation of avian egg weight to body weight.
612 The Auk 92:750-765. doi:10.2307/4084786

613 Seymour RS, Ackerman RA. 1980. Adaptations to underground nesting in birds

and reptiles. American Zoologist 20:437-447. doi:10.1093/icb/20.2.437

Seymour, RS, Vleck D, Vleck CM, Booth DT. 1987. Water relations of buried eggs of mound building birds. Journal of Comparative Physiology B 157:413-422. doi:10.1007/bf00691824

Sibley CG, Monroe BL Jr. 1990. Distribution and Taxonomy of Birds of the World. New Haven, Yale University Press.

Thompson MB, Goldie KN. 1990. Conductance and structure of eggs of Adelie penguins, *Pygoscelis adeliae*, and its implications for incubation. Condor 92:304-312. doi:10.2307/1368228

Trimby P, Grellet-Tinner G. 2011. The hidden secrets of dinosaur eggs revealed using analytical scanning electron microscopy. Infocus Magazine (RSM) 24:4-21.

Tullett S, Board R, Love G, Perrott H, Scott V. 1976. Vaterite deposition during eggshell formation in the cormorant, gannet and shag, and in 'shell-less' eggs of the domestic fowl. Acta Zoologica 57:79-87. doi:10.1111/j.1463-6395.1976.tb00213.x

Vleck D, Vleck CM, Seymour RS. 1984. Energetics of embryonic development in the Megapode birds, Mallee Fowl (*Leipoa ocellata*) and Brush-turkey (*Alectura lathami*). Physiological Zoology 57:444–456. Stable URL: http://www.jstor.org/stable/30163346